Optical Materials 33 (2010) 107–111

Contents lists available at ScienceDirect

Optical Materials

journal homepage: www.elsevier.com/locate/optmat

Increased Er^{3+} upconversion in tellurite fibers and glasses by co-doping with Yb^{3+}

J. Jakutis [a,*], L. Gomes [a], C.T. Amancio [b], L.R.P. Kassab [b], J.R. Martinelli [c], N.U. Wetter [a]

[a] Centro de Lasers e Aplicações, IPEN-SP, 05508-000 São Paulo, SP, Brazil
[b] Laboratório de Vidros e Datações, FATEC-SP, 01124-060 São Paulo, SP, Brazil
[c] Centro de Ciência e Tecnologia de Materiais, IPEN-SP, 05508-000 São Paulo, SP, Brazil

ARTICLE INFO

Article history:
Received 23 February 2010
Received in revised form 17 July 2010
Accepted 25 August 2010
Available online 24 September 2010

Keywords:
Tellurite glasses
Optical spectroscopy
Glass fibers
Rare earth doped glasses

ABSTRACT

We report infrared-to-visible frequency upconversion in Er^{3+}–Yb^{3+} co-doped TeO_2–GeO_2–PbO glasses and fibers. The upconversion is investigated as a function of the co-doping with different Yb^{3+} concentration. We observe an increase of the green and red upconversion intensities of up to 400 times with increasing Yb^{3+} concentration and explain the mechanism involved in the energy transfer process. The pump source is a diode laser emitting at 980 nm in resonance with the $^2F_{7/2} \rightarrow {}^2F_{5/2}$ transition. The tellurite glasses have a relatively low phonon energy (~700 cm^{-1}) among oxides, high refractive index (~2), large transmission window (350 nm–6500 nm) and can be easily pulled into fibers. We also characterized fibers obtained from these compositions and measured similar characteristics when compared to bulk glasses.

1. Introduction

Glasses based on TeO_2 are transparent in the visible, near and mid infrared regions. The position of the IR cut-off may be shifted towards longer wavelength as heavier ions enter the glass composition in binary and ternary systems. Compared to other oxide glasses, tellurite compositions have low phonon energy and show high nonlinearity because of their high refractive index (~2.0). These two characteristics yield low non-radiative decay rates and high radiative emission rates of rare-earth energy levels. As a result, these glasses can provide efficient upconversion luminescence intensities. In particular, TeO_2–GeO_2–PbO glasses have a transmission window ranging from 0.36 μm to 6.5 μm and phonon energy of 700 cm^{-1}, similar to germanate glasses but lower than silicates (1100 cm^{-1}) and phosphates (1200 cm^{-1}) [1]. For example, hosts based on fluoride systems have been used for developing infrared laser pumped solid state upconversion lasers, due to their lower phonon energy [2]. Another essential property of above tellurite composition is its suitability to be pulled in the form of a fiber [3]. Er^{3+} doped glasses have attracted much interest due to their important optical properties used in lasers [4], optical amplifiers [5], photonic devices and as infrared sensors. With the development of high power 980 nm laser diodes, these interests were stimulated from the application point of view. The spectral region of the $^2F_{7/2} \rightarrow {}^2F_{5/2}$ transition of the Yb^{3+} ion overlaps that of the $^4I_{15/2} \rightarrow {}^4I_{11/2}$ transition of the Er^{3+} ion providing an effective Yb^{3+} to Er^{3+} transfer mechanism of the excitation energy [6]. Tellurite glasses co-doped with Yb^{3+}, Er^{3+} and Eu^{3+} have been studied [7] and intense white emission has been shown when adding Pr^{3+} to the system [8].

We produced and characterized, for the first time, five samples of Er^{3+}/Yb^{3+} co-doped tellurite glasses with the above mentioned composition of 0.5 wt.% of Er_2O_3 and 1.0–5.0 wt.% of Yb_2O_3 and one with 1.0 wt.% of Er_2O_3 only. We observe an increase of the green and red upconversion intensities when the concentration of Yb^{3+} increases in the bulk material, being the increase of the red emission stronger than the green one. An important characteristic of this composition is its ability to be pulled in fibers, maintaining thereby the same characteristics as its bulk material, which enables its integration into photonic devices.

2. Experimental

2.1. Preparation of glasses

Samples were prepared adding 0.5 wt.% of Er_2O_3 and different concentrations of Yb_2O_3 (1–5 wt.%) to the following composition: $33.33TeO_2$–$33.33GeO_2$–33.33PbO (T1), in wt.%. A total of 12 g of powder was melted for 1 h in a platinum crucible at 1050 °C, quenched in air atmosphere in heated brass moulds, annealed for 1 h at 350 °C (considering the transition temperature) and then cooled to room temperature inside the furnace. The glasses were prepared with high purity (99.999%) oxides. Special care was taken during the preparation in order to avoid the contamination with other rare-earth and to reduce the incorporation of OH^- by minimizing the time taken to mix the powders.

* Corresponding author. Tel.: +55 11 94519464.
E-mail addresses: jonasjakutis@gmail.com (J. Jakutis), nuwetter@ipen.br (N.U. Wetter).

0925-3467/$ - see front matter © 2010 Elsevier B.V. All rights reserved.
doi:10.1016/j.optmat.2010.08.021

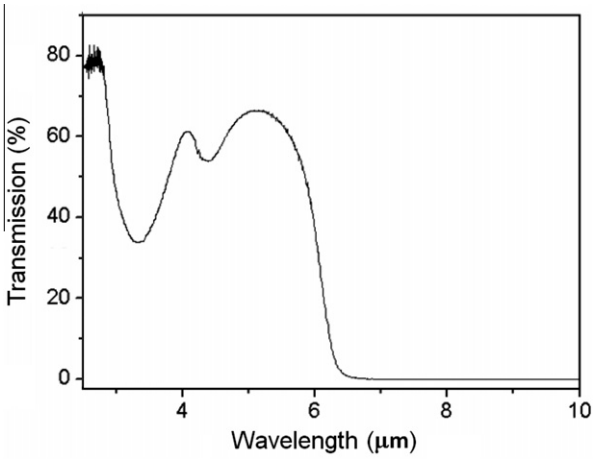

Fig. 1. Transmission spectrum of an undoped TeO_2–GeO_2–PbO glass.

The samples produced are colorless, homogeneous, stable against crystallization and non-hygroscopic. Finally, the samples were polished for absorption and emission measurements. Fig. 1 shows the transmission spectrum for an undoped bulk sample with thickness of 2 mm.

Visible emission was obtained with 3 W of pulsed (50% duty cycle) diode laser excitation at 960 nm, dispersed by a monochromator and collected by an S-20 photomultiplier. All measurements were made at room temperature.

2.2. Fiber pulling

The fibers were obtained by a manual pulling process. The glass (bulk) was melted again in a platinum crucible. Then, the temperature was slowly decreased until the viscosity of the melt became appropriate for pulling glass fibers manually. Fibers were pulled continuously by touching the liquid surface with the tip of a silica rod moving upwards using constant speed.

In the experiments we used a fiber of 2 cm length and constant diameter of approximately 100 μm and recorded the fluorescence that escapes perpendicularly to the fiber at 90° (Fig. 2). The pump light is channeled down the fiber by total internal reflection because of its high index of refraction (~2.0) and the fact that this fiber is not in contact with any other material than air. Due to its large refractive index, the numerical aperture of this fiber is also much larger than the pump light divergence. The pump light is completely absorbed by the Er^{3+} and Yb^{3+} ions in the first few millimeters which can be observed by the fact that the green luminescence originates only from the pumped end of the fiber.

3. Theory

Based on the schematic energy level diagram of Fig. 3, below rate equations are obtained for the Er^{3+}/Yb^{3+} system considering cw pumping at 960 nm (Yb^{3+}). n_1 and n_2 are the populations of $^2F_{7/2}$ and $^2F_{5/2}$, respectively. n_3, n_4, n_5, n_6 and n_7 are the $^4I_{15/2}$, $^4I_{13/2}$, $^4I_{11/2}$, $^4F_{9/2}$ and $^4S_{3/2}$ populations of Er^{3+} considering only the most important and relevant energy levels participating in the upconversion processes involved.

The rate equations comprised in the model use normalized populations n_i for Er^{3+} and Yb^{3+}.

$$\frac{dn_3}{dt} = -K_1 n_2 n_3 + \frac{\beta_{53}}{\tau_{R5}} n_5 + \frac{n_4}{\tau_4} \tag{1}$$

$$\frac{dn_5}{dt} = K_1 n_2 n_3 - K_2 n_2 n_5 - \frac{n_5}{\tau_5} \tag{2}$$

$$\frac{dn_6}{dt} = K_3 n_2 n_4 - \frac{n_6}{\tau_6} \tag{3}$$

$$\frac{dn_7}{dt} = K_2 n_2 n_5 - \frac{n_7}{\tau_7} \tag{4}$$

where the β_{ij} represent the luminescence branching ratios and the τ_{Ri} are the radiative lifetimes of the excited states of Er^{3+} labeled as $i = 3$, 4, 5, 6 and 7. The steady state condition $dn_i/dt = 0$ gives the following populations of interest: $n_4 = \tau_4(K_1 n_2 i_3 - \beta_{53} n_5/\tau_5)$, $n_5 = K_1 n_2 n_3/(K_2 n_2 + 1/\tau_5)$, $n_6 = \tau_6 K_3 n_2 n_4$ and $n_7 = \tau_7 K_2 n_2 n_5$. Using the assumption that $K_2 n_2 > > 1/\tau_5$, one obtains $n_5 = n_3 K_1/K_2$ and n_6 and n_7, responsible for the 660 nm and 550 nm luminescence, given by $n_6 = \tau_6\tau_4 K_1 K_3 n_2^2 n_3 - \tau_6\tau_4 n_2 n_3 \beta_{53} K_1 K_3/(\tau_5 K_2)$ and $n_7 = \tau_7 K_1 n_2 n_3$. Using that K_i has a linear dependence on [Yb] concentration

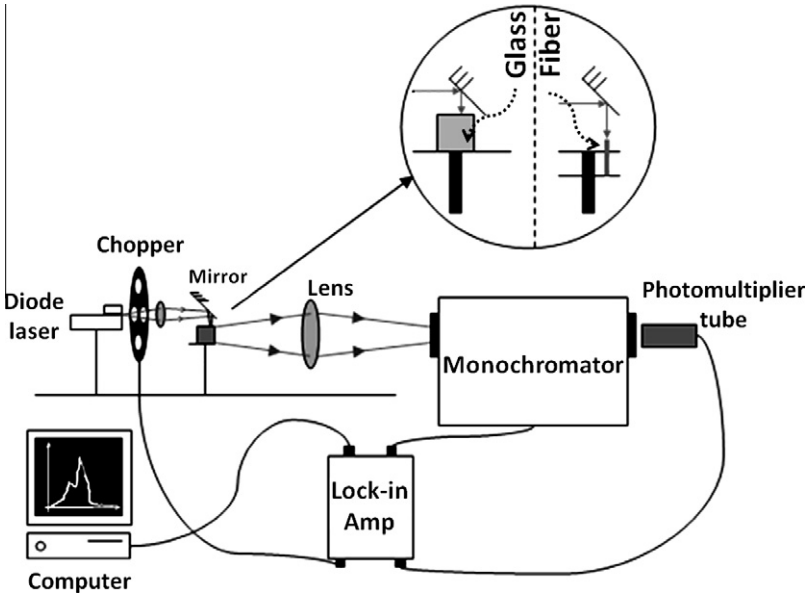

Fig. 2. System used for emission measurements.

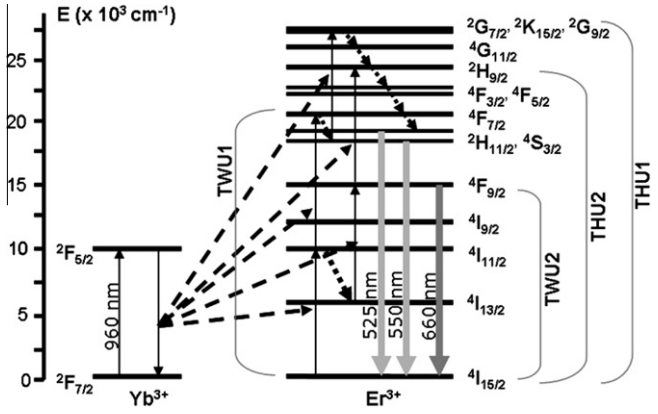

Fig. 3. Energy level scheme of a co-doped system with Er^{3+}/Yb^{3+}.

(hopping or diffusion model), we obtain $n_6 = c_1[Yb]^2$-$c_2[Yb]$ and $n_7 = c_3[Yb]$, where c_1, c_2 and c_3 are constants that are independent of the ytterbium concentration.

4. Results

Five co-doped glasses and a pure Er_2O_3 doped samples were measured in the bulk and in the fiber. Increase of the Yb_2O_3 concentration caused an enhancement of the upconversion emissions in the visible region as shown in Figs. 4 and 5. There are two main emission peaks in the green and in the red spectral region around 550 nm and 660 nm, respectively. Comparing the single doped sample (Fig. 5) with the co-doped samples (Fig. 4), an increase of 400 times in the upconversion emission intensity at the green wavelength can be observed for the sample containing 5.0 wt.% of Yb_2O_3. In all cases the green emission is stronger than the red emission, the latter being almost absent in the singly doped sample (Fig. 5). The green emission can be further separated into two peaks, one at 525 nm and another at 550 nm. To compare the emission bands, we integrated the area beneath each emission as shown in Fig. 6.

In all cases an enhancement of the emission with increasing Yb_2O_3 concentration is seen. The emission is always stronger at 550 nm than at 660 nm and at 525 nm. The results show that the red emission increases more as a function of Yb_2O_3 concentration than does the green emission. This demonstrates that Yb^{3+} ions are playing an important role in the energy transfer process and

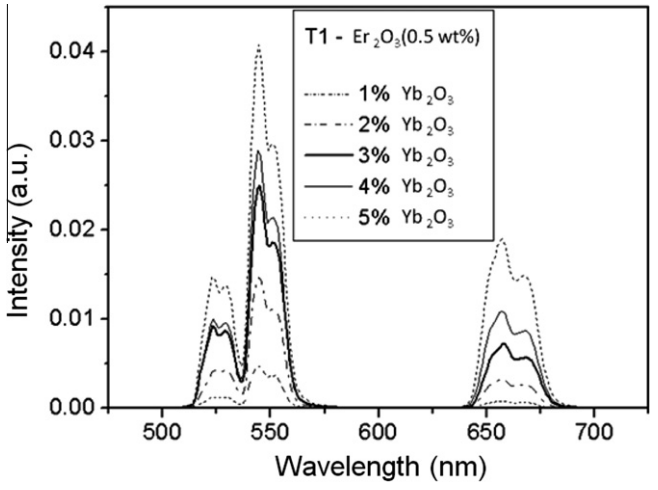

Fig. 4. Frequency upconversion spectra of co-doped T1 glasses.

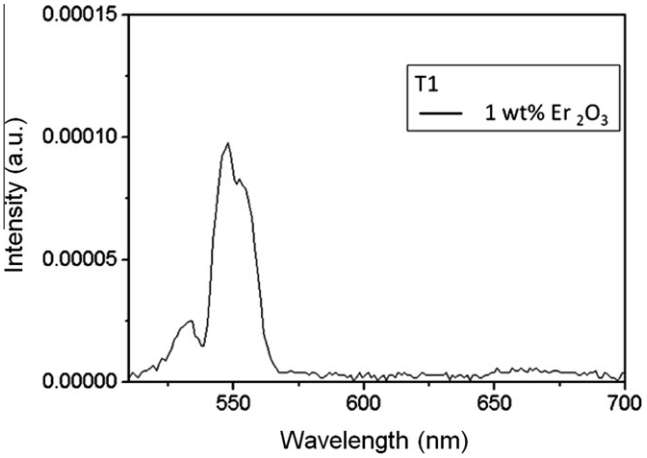

Fig. 5. Frequency upconversion spectrum of Er_2O_3 single doped T1 glass.

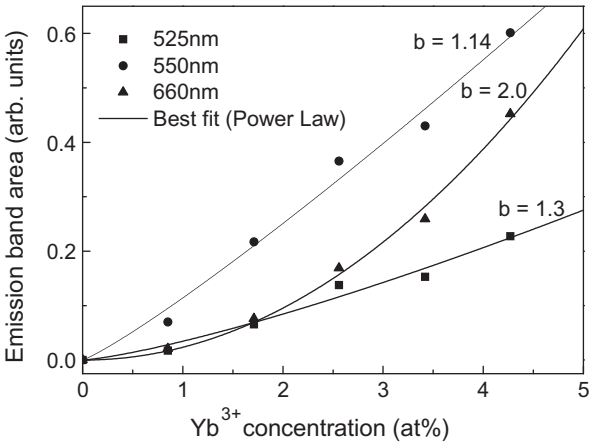

Fig. 6. Integrated emission band of the three upconversions as a function of the Yb_2O_3 concentration and fitting parameters.

that the influence of a higher Yb^{3+} concentration is predominant in the red emission. Best fit was achieved using a power law function $I = a[Yb]^b$. Best fitting parameters obtained are: (i) $b = 1.3$ for 525 nm luminescence; (ii) $b = 1.14$ for 550 nm; (iii) $b = 2.0$ for 660 nm. The power factor $b \sim 1$ is expected for a migration assisted energy transfer (hopping or diffusion model). In this case the transfer rate is given by $K = 20c_Ac_D(C_{DA}C_{DD})^{1/2}$, where c_A is the acceptor concentration (Er) and c_D is the donor concentration (Yb) [9]. The constants C_{DD} and C_{DA} are the transfer constants given in cm^6/s due to the donor–donor and donor–acceptor, respectively. The investigation on the 660 nm luminescence intensity has shown a quadratic dependence on the ytterbium concentration, which can be explained using the rate equations involved in the T1, T2 and T3 upconversion Er processes given in the theory section.

In a frequency upconversion process, the emitting level population increases as a function of the pump intensity, the exponent of the intensity depending on the number of absorption steps that occurred, type of upconversion (e.g. excited state absorption, energy transfer upconversion) and type of depletion (linear decay or depletion by upconversion) [10]. The relevant exponents for the 550 nm and 660 nm emissions for the different concentrations of Yb_2O_3 can be found in Fig. 7.

The results demonstrate that the higher the Yb_2O_3 concentration the higher the upconversion efficiency and the smaller the exponent for both, green and red emissions. As shown in Fig. 3,

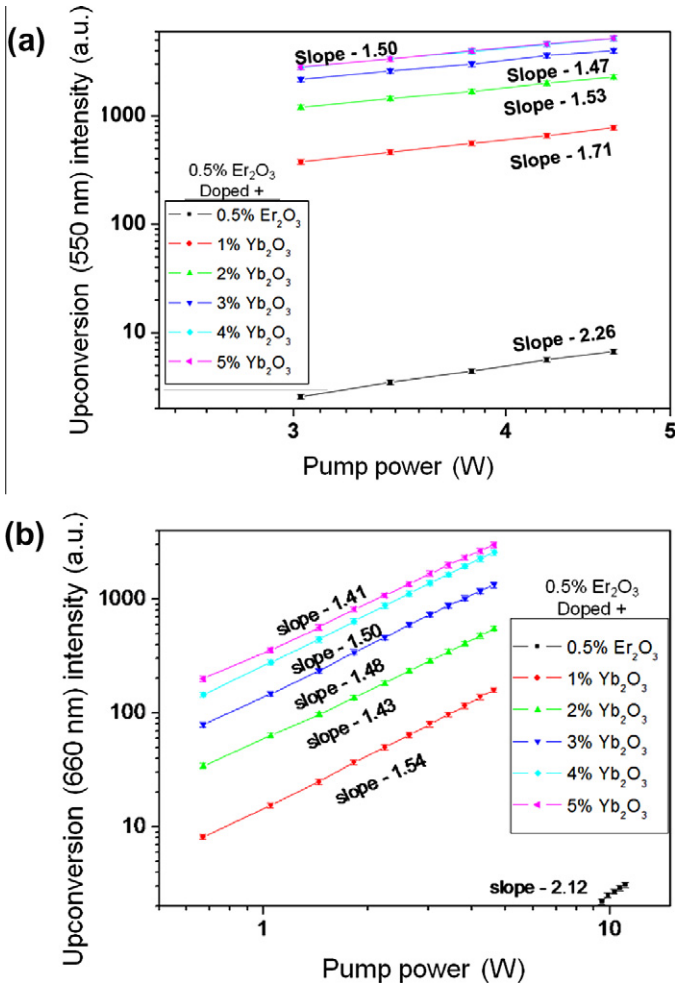

Fig. 7. Emission intensity versus pump power intensity for the 550 nm (a) and 660 nm (b) emissions, in log–log scale.

the Er/Yb co-doped system generally involves two or three upconversion steps. The more depletion by upconversion exists when compared to linear decay, the lower the exponent [10].

As shown in Fig. 8, the fibers pulled from the melt show the same behavior as a function of Yb^{3+} concentration observed for the bulk samples and maintain the same spectral profile.

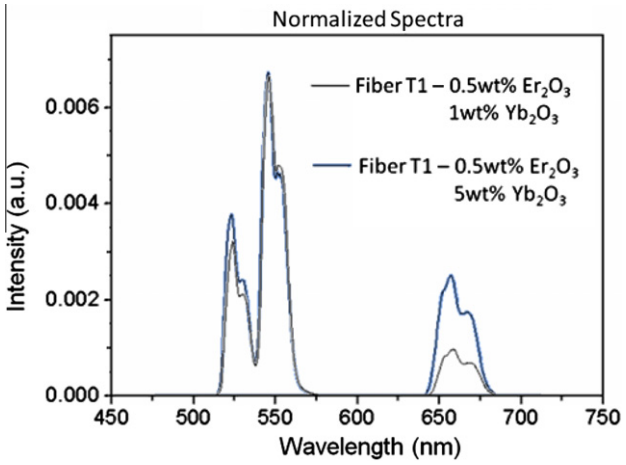

Fig. 8. Upconversion emissions for the fiber samples with the same concentration of Er_2O_3 and different concentrations of Yb_2O_3, 5 wt.% and 1 wt.% of Yb_2O_3.

5. Discussions

Energy transfer occurs in this system mainly by means of a spectral overlap between the $^2F_{7/2} \rightarrow {}^2F_{5/2}$ transition of Yb^{3+} and the $^4I_{15/2} \rightarrow {}^4I_{11/2}$ transition of Er^{3+} (see Fig. 3). The most important two photon upconversion processes in Er^{3+} are TWU1 (two photon upconversion 1) and TWU2 (two photon upconversion 2). The three photon upconversions THU1 and THU2 are feasible for higher pump intensities [13]. After upconversion the following three radiative transitions may occur: $^4H_{11/2} \rightarrow {}^4I_{15/2}$ (525 nm), $^4S_{3/2} \rightarrow {}^4I_{15/2}$ (550 nm) and $^4F_{9/2} \rightarrow {}^4I_{15/2}$ (660 nm). Our results show that the exponent of the co-doped system is always smaller than 2 and therefore, the system involves mainly sequential absorption of two photons for the red and green emissions [11]. Due to the much higher absorption cross section of the Yb^{3+} ions at 960 nm, when compared to Er^{3+}, the upconversion process is mainly based on energy transfer from Yb^{3+} to Er^{3+} with only a small contribution of direct pump absorption by Er^{3+} [12–14]. From the discussion in the result section it follows that the observed decrease of the exponent with higher Yb_2O_3 concentration demonstrates a decrease of the linear decay rate, as shown in Fig. 7(a), indicating a more efficient upconversion. A similar behavior was observed in Fig. 7(b) for the 660 nm emission.

The experimental evidence of the enhancement of the red emission, when compared to the green, for higher Yb^{3+} concentrations can be explained considering the population mechanism of the $^4F_{9/2}$ level by the second transfer channel (TWU2 in Fig. 3). This non-resonant mechanism involves the interaction between the Yb^{3+} excited state and the first Er^{3+} excited multiplet, $^2F_{5/2} \rightarrow {}^2F_{7/2}$ (Yb^{3+}): $^4I_{13/2} \rightarrow {}^4F_{9/2}$ (Er^{3+}) and therefore depends on Yb^{3+} concentration. The energy mismatch of this process is approximately 1000 cm^{-1} [15] and it has been previously reported to occur in Er^{3+}/Yb^{3+} co-doped phosphate glasses [12] and in oxyfluoride glasses [13]. This second mechanism provides a direct path for populating the $^4F_{9/2}$ level from where the red emission originates. One crucial step in this mechanism is the non-radiative decay from the $^4I_{11/2}$ level to the $^4I_{13/2}$ level which depends on the phonon energy [16]. For this reason, the effect is even more intense in silicate oxyfluoride Er^{3+}/Yb^{3+} co-doped glasses [13] because of their higher phonon energy (~1100 cm^{-1}) when compared to tellurite glasses and germanate glasses (700–800 cm^{-1}) [14]. The same effect was reported for germante glasses in the literature [17].

Not all glasses can be pulled into fibers; principally high index glasses as the one reported in this work. Secondly, in some cases it is possible to pull the fiber from the glass matrix but not from the co-doped glass composition. Besides, spectroscopic properties might change strongly from the bulk glass to the fiber. This specific glass composition has the capability to pull fibers from bulk without loss of its optical qualities (Figs. 4 and 8). Also, being an amorphous glass matrix with the capability of pulling fibers, it should be possible to fabricate fibers with cladding in future works.

6. Conclusions

An enhancement of 400 times in the green Er^{3+} upconversions has been demonstrated in the presence of 5% Yb^{3+} ions for tellurite glasses and fibers. The red Er^{3+} emission increased more than the green emission with higher Yb_2O_3 content. Pump power dependent studies revealed that both, green and red emissions resulted from two photon upconversion processes. The best fittings of the 660 nm and 550 nm luminescence are in agreement with the n_6 and n_7 populations behavior obtained using the rate equations system for Er^{3+} in Yb/Er doped telluride glasses pumped by cw laser at

960 nm, where the Yb–Er transfers (T1, T2 and T3) are dependent on the ytterbium concentration.

Successful experiments with fiber pulling indicate that these glasses should prove to be an excellent option for optical applications such as photonic devices, infrared sensors and also fiber amplifiers.

Acknowledgements

The authors thank Fundação de Amparo à Pesquisa de São Paulo (FAPESP) and Conselho Nacional de Desenvolvimento Científico e Tecnológico (CNPq).

References

[1] X. Zou, T. Izumitani, Journal of Non-Crystalline Solids. 162 (1993) 68.
[2] S.A. Pollack, D.B. Chang, Journal of Applied Physics 64 (1988) 2885.
[3] J.S. Wang, E.M. Vogel, E. Snitzer, Optical Materials 3 (1994) 187.
[4] O. Toma, E. Osiac, S. Georgescu, Optical Materials 30 (2007) 181.
[5] J.T. Ahn, K.H. Kim, IEEE Photonics Technology Letters 16 (2004) 84.
[6] V.P. Gapontsev, S.M. Matisin, A.A. Iseneev, V.B. Kravchenko, Erbium Glass Lasers and Their Applications Optics and Laser Technology 14 (1982) 189.
[7] Y. Dwivedi, A. Rai, S.B. Rai, Journal of Luminescence 129 (2009) 629.
[8] Y. Dwivedi, A. Rai, S.B. Rai, Journal of Applied Physics 104 (2008) 043509.
[9] R.C. Powell, Physics of Solid State Laser Materials, Springer, New York, 1998.
[10] M. Pollnau, D.R. Gamelin, S.R. Luthi, H.U. Gudel, Physical Review B 61 (2000) 3337.
[11] L.R.P. Kassab, A.D. Preto, W. Lozano, F.X. Sá, G.S. Maciel, Journal of Non-Crystalline Solids 351 (2005) 3468.
[12] F. Song, G. Zhang, M. Shang, H. Tan, J. Yang, F. Meng, Applied Physics Letters 79 (2001) 1748.
[13] L. Feng, J. Wang, Q. Tang, H. Hu, H. Liang, Q. Su, Journal of Non-Crystalline Solids 352 (2006) 2090.
[14] G. Qin, W. Qin, C. Wu, D. Zhao, J. Zhang, S. Lu, S. Huang, W. Xu, Journal of Non-Crystalline Solids 347 (2004) 52.
[15] E. Cantelar, F. Cussó, Journal of Luminescence 102 (2003) 525.
[16] Z. Shang, G. Ren, Q. Yang, C. Xu, Y. Liu, Y. Zhang, Q. Wu, Journal of Alloys and Compounds 460 (2007) 539.
[17] F.A. Bomfim, J.R. Martinelli, L.R.P. Kassab, N.U. Wetter, J.J. Neto, Journal of Non-Crystalline Solids 354 (2008) 4755.